10668 J. Agric. Food Chem. 2010, 58, 10668–10676
DOI:10.1021/jf1017934

JOURNAL OF AGRICULTURAL AND FOOD CHEMISTRY
ARTICLE

Inhibition of Pancreatic Elastase by Polyphenolic Compounds

Natércia F. Brás,[†] Rui Gonçalves,[‡] Nuno Mateus,[‡] Pedro A. Fernandes,[†] Maria João Ramos,[†] and Victor de Freitas*,[‡]

[†]REQUIMTE, Departamento de Química, Faculdade de Ciências, Universidade do Porto, Rua do Campo Alegre, 687, 4169-007 Porto, Portugal, and [‡]Centro de Investigação em Química, Departamento de Química, Faculdade de Ciências, Universidade do Porto, Rua do Campo Alegre, 687, 4169-007 Porto, Portugal

Polyphenols are plant secondary metabolites commonly present in the human diet that possess the ability to bind and inhibit digestive proteins. In the present study, kinetic measurements of porcine pancreatic elastase (PPE) activity were determined using Suc-$(Ala)_3$-*p*-nitroanilide as substrate and polyphenolic compounds as inhibitors. A positive relationship between the degree of polyphenol polymerization and the capacity of the polyphenols to inhibit PPE was observed. Procyanidins with a molecular weight of at least 1154 Da were necessary to observe a significant inhibitory ability. Kinetic parameters were also calculated and confirmed that the inhibition is reversible and competitive. Molecular docking and dynamics simulations demonstrated that the tetramer structure has a higher affinity to the enzyme due the establishment of more contact points with the amino acids present in its active site. Hydrogen bond interactions and hydrophobic effects established between the polyphenol groups and the side chain of residues stabilize and favor the binding mode of this procyanidin. This work is relevant to the study of the antinutritional effects caused by dietary tannins on the digestive enzymes' activity, reducing food digestibility and the absorption of nutrients. In general, the elastase model studied herein allows a better understanding of the inhibitory ability of polyphenol compounds.

KEYWORDS: Procyanidins; pancreatic elastase; antinutritional effect; competitive inhibitor; binding free energy

INTRODUCTION

Some beverages such as wine, tea and berry juices are the main dietary sources of polyphenols with reported health benefits (*1*). It is known that these compounds possess many biological and pharmacological properties, such as reducing the risk of cancer and heart diseases, and acting as natural antioxidants in the food industry (*2*−*4*). Some authors have studied these properties using computational methodologies (*5*, *6*).

Dietary polyphenols show a wide diversity of structures subdivided in two broad classes of tannins: condensed tannins (proanthocyanidins, which are flavan-3-ol units with various degrees of substitution and polymerization) and hydrolyzable tannins (gallic or ellagic esters of glucose) (*1*). As condensed tannins are large polymeric structures, they are poorly absorbed in the intestine and remain in the digestive tract for a long time (*7*). Moreover, various studies show that these polyphenol complexes can react and/or bind proteins, acting as complexation or precipitation agents with biological activity in the digestive tract (*8*−*10*). Thus, it was suggested that the binding of polyphenols could denature enzymes and lead to the loss of their catalytic activity. These interactions have a hydrophobic and hydrogen bonding nature and could result in insoluble aggregates that precipitate (*11*). Therefore, this complexation ability can result in the inhibition of digestive enzymes such as lipases, glycosidases and proteases, reducing food digestibility. Taking into account the reduced absorption occurring in polyphenol-rich diets, the interest in studying the inhibition of digestive enzymes by these compounds has increased in the past few years.

It is well-known that some polyphenols may inhibit the activity of proteolytic enzymes, which have crucial biological effects on disease processes, such as bacterial colonization, tumor invasion, and metastasis (*12*). Green tea (−)-epigallocatechin-3-gallate (EGCG) has been found to be responsible for growth inhibition and regression of human prostate tumor in athymic nude mice (*4*). Catechins, the polyphenolic compounds most abundant in tea leaves and grape seeds, have already been found to inhibit various metallo- and serine-proteases crucial for some processes like inflammation, angiogenesis and cancer survival, such as leukocyte elastase and gelatinases (*13*). Moreover, it has also been reported that some phenolic compounds possess the ability to inhibit the proteasome, a multicatalytic protease responsible for the degradation of most cellular proteins. Tea polyphenols (−)-epigallocatechin gallate and (−)-epicatechin-3-gallate have been pointed out to greatly inhibit the proteasomal chymotrypsin-like activity (*14*).

Although various studies have shown that polyphenols can prevent disease, the exact mechanism by which this occurs is not well understood. Polyphenol complexation with proteins has been studied in solution by NMR spectroscopy (*15*−*17*), microcalorimetry (*18*), enzyme inhibition (*19*), protein precipitation (*11*), turbidity (*20*), nephelometry (*11*) and fluorescence quenching (*8*, *10*). Elastases are serine proteases that degrade a wide variety of protein

*Author to whom correspondence should be addressed. E-mail: vfreitas@fc.up.pt. Tel: +351 220 402 558. Fax: +351 402 659.

 Published on Web 09/14/2010

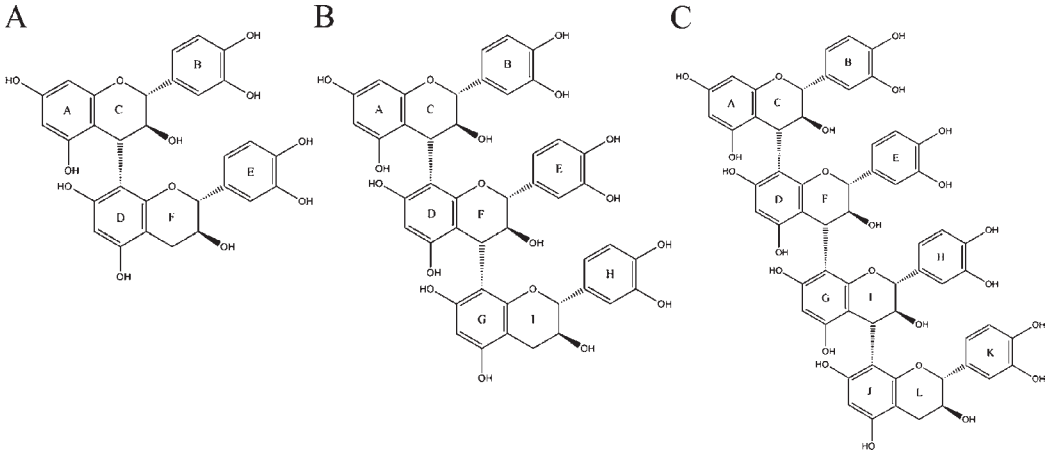

Figure 1. Representation of the dimer B3 (**A**), trimer C2 (**B**) and tetramer (**C**) structures.

substrates including the connective tissue protein elastin (*21*). Human neutrophil elastase (HNE) and porcine pancreatic elastase (PPE) represent two of these elastin-cleaving enzymes. PPE is secreted into the small intestine and is essential for digestion of proteins rich in connective tissues, while HNE is involved in phagocytosis and defends against infection. HNE also participates in the controlled proteolysis of elastic fibers during normal growth and remodeling (*12*). However, under certain pathological conditions the activity of these enzymes can lead to major, uncontrolled destruction of structural proteins and to severe diseases like pulmonary emphysema, acute pancreatitis, rheumatoid arthritis, thrombosis and stroke (*12*, *13*). Bearing their crucial therapeutic importance, the high structural similarity of both enzymes, and the fact that PPE is directly accessible to polyphenols due to its action in the digestive tract, the inhibitory ability of procyanidins on pancreatic elastase should be explored. PPE (E.C. 3.4.21.36) is a multispecific serine protease composed of 240 amino acids in its active state. As all serine protease family members, it has a conserved active site catalytic triad formed by serine, histidine, and aspartate residues (*22*). Porcine and rat elastases cleave substrates at peptide bonds involving a small hydrophobic amino acid (preferentially Ala) and another residue of any kind (Ala−X bonds) (*21*). Some authors have studied the inhibitory effects on mouse, porcine and human pancreatic elastase of structurally different inhibitors, such as soybean trypsin inhibitor, lima bean trypsin inhibitor, ovomucoid, serine proteinase inhibitor phenylmethanesulfonyl fluoride, elastatinal, benzamidine, bovine pancreatic trypsin inhibitor, leupeptin and human β-casomorphin-7 (*21*, *23*, *24*). In a previous work, procyanidin complexation with PPE has been studied by fluorescence quenching, circular dichroism, nephelometry, and dynamic light scattering, as well as computational methodologies (*25*).

This work aims to study the effect of procyanidins dimer B3, trimer C2, a tetramer and an oligomeric fraction of procyanidins (OFP) on the hydrolysis of Suc-$(Ala)_3$-*p*-nitroanilide by PPE. **Figure 1** shows the structures of the dimer B3, trimer C2 and a tetramer. The inhibition constants (K_i) for procyanidins trimer C2, tetramer and OFP were determined. Computational calculations, namely, molecular docking and molecular dynamic simulations, with the substrate, trimer and tetramer molecules bound to the active site of the enzyme were also performed.

MATERIALS AND METHODS

Materials. Porcine pancreatic elastase and Suc-$(Ala)_3$-*p*-nitroanilide substrate were obtained from Sigma Aldrich and stored at −20 °C. Both elastase and substrate were dissolved at room temperature in phosphate buffer (0.1 M, pH 7.0) and frozen.

Synthesis of Dimeric, Trimeric and Tetrameric Procyanidins. The synthesis of procyanidin dimers, trimers and tetramers followed the procedure described in the literature (*26*, *27*). For the synthesis of dimers, taxifolin (200 mg) and catechin (575 mg) were dissolved in ethanol under argon atmosphere (taxifolin/catechin ratio 1:3). The mixture was then treated by dropwise addition of sodium borohydride (in ethanol). The pH was then lowered to 4.5 by slowly adding 50% aq CH_3COOH, and the mixture was allowed to stand under argon atmosphere for 30 min. The reaction mixture was extracted with ethyl acetate. After evaporation of the solvent, water was added and the reaction mixture was passed through reverse-phase C18 gel, thoroughly washed with water and eluted with methanol. The obtained fraction, after evaporation of methanol, was passed through a TSK Toyopearl HW-40(s) gel column (300 mm × 10 mm i.d., with 0.8 mL min^{-1} methanol as eluent) coupled to a UV−vis detector. Several fractions corresponding to the eluted peaks in **Figure 2** were collected and analyzed by ESI-MS infusion in the negative mode (Finnigan DECA XP PLUS) yielding procyanidin dimer B3 ($[M - H]^-$ at m/z = 577); procyanidin trimer C2 ($[M - H]^-$ at m/z = 865) and procyanidin tetramer ($[M - H]^-$ at m/z = 1153). For the production of trimer and tetramer the ratio of taxifolin to catechin were changed to (1:1) and (1:0.5) respectively to favor the more polymerized products (trimers and tetramers).

The identity of both dimer B3 and trimer C2 was confirmed by NMR (*28*, *29*). Regarding the tetramer its characterization by NMR has proven to be difficult due to the presence of several rotamers that complicate signal attribution. However the tetramer used was the more abundant that probably corresponds to the fully C4−C8 linked isomer since this interflavanoid linkage is more likely to occur than C4−C6.

Oligomeric Procyanidin Fraction. Oligomeric procyanidins were obtained as described in the literature (*30*). Briefly, *Vitis vinifera* grape seeds were extracted in ethanol/water/chloroform (1:1:2). The hydroalcoholic phase was extracted with ethyl acetate and evaporated yielding a residue composed of monomeric and oligomeric procyanidins (OFP). In order to obtain a purified fraction corresponding to the oligomeric procyanidins, the residue was fractionated through a TSK Toyopearl HW-40(s) gel column (100 mm × 10 mm i.d., with 0.8 mL min^{-1}). Fraction I corresponding to catechin monomers and low M_w procyanidins was eluted with methanol for the first 6 h; fraction II containing more polymerized procyanidin oligomers (OPF) was obtained after elution with methanol/CH_3COOH (95:5, v/v) during the next 14 h; more polymerized procyanidins were not eluted. Fractions were mixed with deionized water and freeze-dried. The procyanidin composition of each fraction was determined through ESI-MS (Finnigan DECA XP PLUS) as described elsewhere (*31*). Fraction II, the one used in the study, contains procyanidin oligomers up to hexameric molecules: dimer (MW = 578); dimer gallate (MW = 730); trimer (MW = 866); trimer gallate (MW = 1018); tetramer (MW = 1154); tetramer gallate (MW = 1306); pentamer gallate (MW = 1595); hexamer gallate (MW = 1882).

Enzymatic Activity Assays. Elastase activity was assayed using Suc-$(Ala)_3$-*p*-nitroanilide as substrate. This substrate was chosen because it is specific to the proteolytic activity of pancreatic elastase, and it was used in similar works present in the literature (*21*, *23*, *32*). After protease

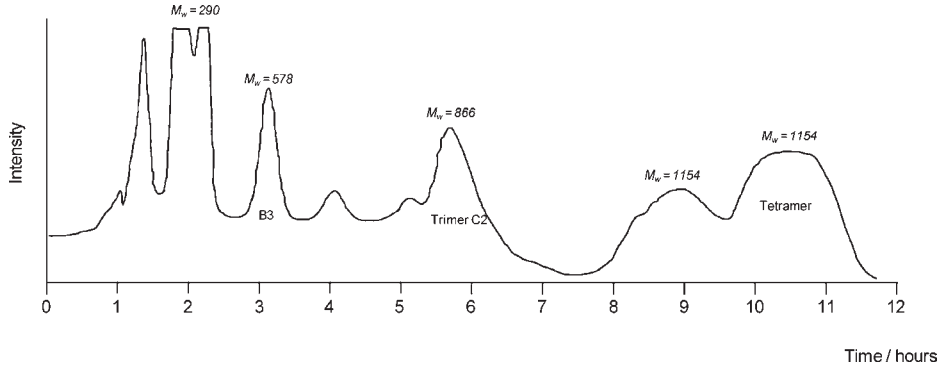

Figure 2. Chromatogram (280 nm) obtained from Toyopearl HW-40(s) gel column chromatography of the reaction products corresponding to the hemysinthesis of procyanidins. Values above representative peaks correspond to the molecular mass of the compound as determined by ESI-MS.

action this substrate releases *p*-nitroaniline, which is detectable by spectrophotometry at 405 nm using a UV−vis microplate reader (Biotek Powerwave XS) and appropriate data processing software (KC4). The kinetic parameters K_m and V_{max} of the enzyme were determined using the same substrate. Several concentrations of the substrate, from 10 to 900 μM, were tested at 0.8 μM of elastase. This range of concentrations has proven to be appropriate to calculate the initial rate from the graphs of $\Delta Abs = f(time)$ in the experimental conditions used. In each well of a 96 well (300 μL) microreader plate 20 μL of elastase working solution was mixed with different volumes of procyanidin solution (phosphate buffer 0.1 M, pH 7.0); the total volume before substrate addition was adjusted to 280 μL with phosphate buffer. Previous studies have shown that the optimal pH values of PPE activity vary between 7.0 and 8.8 depending on the buffer used (*21*). Therefore, the assays were conducted at physiological temperature (37 °C) and at the optimal pH (7.0) of elastase in phosphate buffer. After 5 min, a blank was measured and 20 μL of substrate was added to each well. IC_{50} values and the inhibition constants were calculated and used to compare the inhibitory ability of different procyanidins. The Lineweaver−Burk graphs were plotted in the absence and presence of the oligomeric fraction of procyanidins as inhibitor.

Statistical Analysis. All assays were performed in triplicate. The statistical differences were evaluated using analysis of variance (ANOVA); the mean values were compared using a Tukey test, and all statistic data were processed using the SPSS software, version 15.0 (SPSS Inc., Chicago IL).

Computational Studies. The X-ray crystallographic structure of porcine pancreatic elastase was obtained from the database protein databank (1QNJ code at 1.1 Å resolution) (*22*). Various studies have shown the existence of conserved waters in the elastase structure (*33*−*35*). In order to include these conserved crystallographic water molecules in the system, any buried water molecule and the ones forming at least one H bond with the enzyme were maintained. This procedure led us to keep 80 of the water molecules of the crystallographic file and delete 413 water molecules. All hydrogen atoms were added taking into account all residues in their physiological protonation state. In order to release the bad contacts in the crystallographic structure, the protein was minimized in three stages during the initial geometry optimization. First, only the hydrogen atoms were minimized; in a second stage the backbone was also minimized; and finally, the entire system was minimized. About 1500 steps were used for each stage, with the first 500 steps performed using the steepest descent algorithm and the remaining steps carried out using conjugate gradient. A substrate or polyphenolic molecule (depending on the particular case under study) was initially docked into the structure of the unligated protein, simulating the biological complex enzyme:substrate or enzyme:polyphenol. The docking procedure was made with GOLD (*36*), a program that predicts the binding modes of small molecules into protein binding sites. The program is based on a genetic algorithm that is used to place different ligand conformations in the protein binding site, recognized by a fitting points strategy. Three scoring functions are a posteriori available to rank the obtained solutions. As the docking accuracy obtained with all scoring functions is similar, and the ChemScore is up to three times faster when compared with the other, we have been used this scoring function (*37*). Taking into account the lack of information about the polyphenol-binding mode to the active site of elastase, the docking protocol was performed with some distance constraints between crucial catalytic atoms and atoms of the substrate or polyphenols. An important distance constraint (2.0−3.0 Å) was introduced between the hydrogen atom of the hydroxyl group of the catalytic serine and the carbon atom of the substrate where the cleavage should occur (*34*). The best docking solutions were taken as starting structures for the subsequent minimization and Molecular Dynamic (MD) simulations. To calculate the optimized geometries and electronic properties of the substrate and the different polyphenols, to be used later in the parametrization of these compounds, we have used the Gaussian03 suite of programs (*38*) and performed restricted Hartree−Fock (RHF) calculations, with the 6-31G(d) basis set. The atomic charges were further calculated using RESP (*39*). This methodology was chosen to be consistent with that adopted for the parametrization process in Amber 8.0 software (*40*). Molecular dynamics (MD) simulations were performed for each compound, with the parametrization adopted in Amber 8.0 using the Amber 1999 force field (parm99) for the protein and the GAFF force field for the substrate and polyphenols. In these simulations, an explicit solvation model with preequilibrated TIP3P water molecules was used, filling a truncated octahedral box with a minimum 12 Å distance between the box faces and any atom of the protein. Each structure was minimized in two stages: first, the protein was kept fixed and only the position of the water molecules and counterions was minimized; in the second stage, the full system was minimized. Following a 500 ps equilibration procedure, 5 ns MD simulations were carried out, starting with the optimized structures. The Langevin thermostat was used, and all the simulations were carried out in the *NPT ensemble* with periodic boundary conditions (*41*). All MD simulations were carried out using the Sander module, implemented in the Amber 10.0 simulations package (*42*), with the Cornell force field (*43*). Bond lengths involving hydrogens were constrained using the SHAKE algorithm (*44*), and the equations of motion were integrated with a 2 fs time step using the Verlet leapfrog algorithm. The nonbonded interactions were truncated with a 10 Å cutoff. The temperature of the systems was regulated to be maintained at 310.15 K. All of the MD results were analyzed with the Ptraj module of Amber 10.0 (*42*).

The MM_PBSA script (*45*) implemented in Amber 8.0 was used to calculate the binding free energies for all complexes. A postprocessing treatment of the complex was performed by using its structure, and calculating the respective energies for the complex and all interacting components. The binding free energy difference between the elastase:substrate complex and elastase:polyphenol complexes is defined as

$$\Delta\Delta G_{binding} = \Delta G_{binding}(substrate) - \Delta G_{binding}(polyphenol)$$

In each calculation, 100 snapshots of the complexes were extracted every 100 steps for the last 10000 steps of the run. Electrostatic and van der Waals interactions were calculated using the Cornell force field with no cutoff (*43*). The electrostatic solvation free energy was calculated by solving the Poisson−Boltzmann equation with the software Delphi v.4 (*46*, *47*). The accuracy of this method depends on the self-consistency of the model parameters used to solve the finite difference method implemented in Delphi. The key parameters used were based in a detailed study that correlated the effect of the variation of key parameters in several systems with the correspondent computational time (*48*). The nonpolar

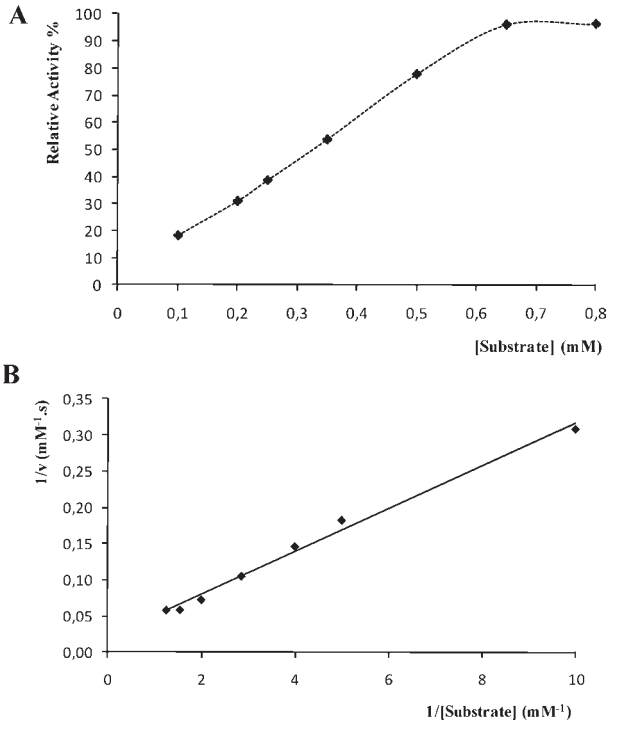

Figure 3. (**A**) Variation of the relative enzymatic activity of porcine pancreatic elastase at 37 °C as a function of Suc-(Ala)$_3$-*p*-nitroanilide concentration. (**B**) Lineweaver−Burk graphic calculated with the same conditions.

contribution to solvation free energy due to van der Waals interactions between the solute and the solvent and cavity formation was modeled as a term that is dependent on the solvent accessible surface area of the molecule. It was estimated using an empirical relation: $\Delta G_{\text{nonpolar}} = o'A + \beta$, where A is the solvent-accessible surface area that was estimated using the molsurf software (*49*). o' and β are empirical constants, and the values used were 0.00542 kcal Å^{-2} mol^{-1} and 0.92 kcal mol^{-1}, respectively. The entropy term was not calculated because it was assumed that its contribution to $\Delta\Delta G_{\text{binding}}$ becomes negligible (*45*). The values of the external and internal dielectric constants used were 80.0 and 1.0, respectively.

RESULTS AND DISCUSSION

Enzymatic Properties of Elastase. The kinetic properties of elastase were already determined in various studies (*21*, *23*, *50*), and it is well-known that this enzyme follows the Michaelis−Menten kinetics. However, it was observed that K_m (Michaelis constant) and V_{max} (maximal velocity) greatly depend on the experimental conditions used, i.e., buffer, pH and temperature. Davril and colleagues obtained a K_m value of 2.0 mM using Suc-(Ala)$_3$-*p*-nitroanilide as substrate in 50 mM Hepes buffer, pH 7.0 and 25 °C (*50*). In this present work, an enzymatic assay based on the hydrolysis of the same substrate was performed, in which the release of *p*-nitroanilide group after hydrolysis was followed over time at 405 nm. The experiments were conducted in 0.1 M phosphate buffer, pH 7.0 and 37 °C. **Figure 3** shows the increment of porcine pancreatic elastase activity with increasing substrate concentrations, as well as the Lineweaver−Burk plot calculated with the same data. A relationship between higher substrate concentrations and larger enzymatic activity was found. The K_m and V_{max} parameters were calculated from the Lineweaver−Burk equation, and the values obtained were 2.09 mM ± 0.46 and 68.25 mM/s ± 13.50, respectively. The kinetic profile was similar to another one obtained in comparable experimental conditions (*50*).

Inhibitory Effect of Polyphenols in Elastase Activity. In order to study the inhibitory effect of procyanidins on elastase activity,

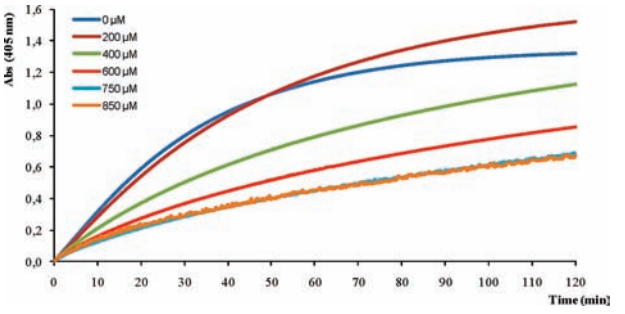

Figure 4. Kinetics activity of elastase (0.8 μM) with increasing concentrations of tetramer procyanidin. Assays were conducted in 0.1 M phosphate buffer (pH 7.0) at 37 °C. The substrate concentration (Suc-(Ala)$_3$-*p*-nitroanilide) used was 250 μM. Each curve is an average of the triplicate analysis.

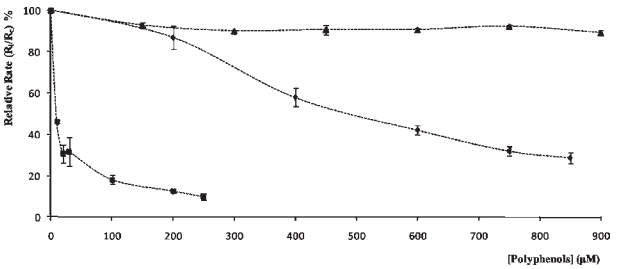

Figure 5. Relative rate of elastase activity (R_i/R_c) at pH 7.0, as a function of procyanidin concentration: ▲ trimer C2, ● tetramer and ■ OFP. Each equation is an average of the triplicate analysis.

assays with different volumes of condensed tannins (dimer B3, trimer C2, tetramer and an oligomeric fraction of procyanidins (OFP) with a higher average molecular weight) were performed.

Figure 4 shows the influence of the tetramer on the protease activity of elastase. In general, the hydrolytic activity decreased with procyanidin concentrations in the case of tetramer, trimer C2 and OFP. However, the procyanidins with lower molecular weight (dimer B3) did not significantly inhibit the activity of elastase (data not shown). The slope of each curve in **Figure 4** corresponds to the hydrolytic rate in the absence of procyanidins (R_c, control assay) and in the presence of several concentrations of procyanidins tested (R_i).

For trimer C2, tetramer and OFP, a plot of relative hydrolysis rate (R_i/R_c) was made using different concentrations from 0 (control assay) to 900 μM (**Figure 5**), and this demonstrates the capacity of each polyphenolic compound to inhibit elastase.

It can be seen from **Figure 5** that procyanidin trimer C2 hardly inhibited the elastase activity (*circa* 10%), while the most polymerized procyanidins (OFP) displayed the highest inhibitory ability (approximately 90%). These results are in agreement with previous studies with other enzymes. It is expected that more polymerized procyanidins establish more van der Waals interactions and hydrogen bonds between their hydrophobic and hydroxyl groups with the side chains of the residues present in the active site. All these results suggest that larger tannins may act as a blocking gate, preventing the substrate access to the active site. Oppositely, as dimer B3 is the smallest procyanidin studied herein, it likely establishes few interactions with the active site and cannot block the cavity, consequently not showing any inhibitory activity.

Furthermore, at the concentration of 750 and 200 μM for tetramer and OFP, respectively, further addition of each procyanidin did not significantly change elastase activity. This residual enzymatic activity may suggest that a population of uninhibited enzyme molecules still subsists and carries on their hydrolytic

Table 1. IC_{50} Values, Inhibitory Constants (K_i), Experimental Binding Free Energies ($\Delta G_{exp.}$) and the Differences in Binding Free Energies of Each Procyanidin Studied Related to the Value Obtained for the Substrate[a]

procyanidins	IC_{50} (μM)	K_i (mM)	ΔG_{exp} (kcal/mol)	$\Delta\Delta G_{exp}$ (kcal/mol)
trimer C2	5863.3 ± 759.8 a	5.237 ± 0.679 a	−3.24 ± 0.08 a	0.56 ± 0.08 a
tetramer	585.1 ± 62.9 b	0.523 ± 0.056 b	−4.66 ± 0.07 b	−0.86 ± 0.07 b
OFP	16.0 ± 0.7 c	0.014 ± 0.001 c	−6.88 ± 0.02 c	−3.07 ± 0.02 c

[a] In each column values with different letters are significantly different ($P < 0.05$).

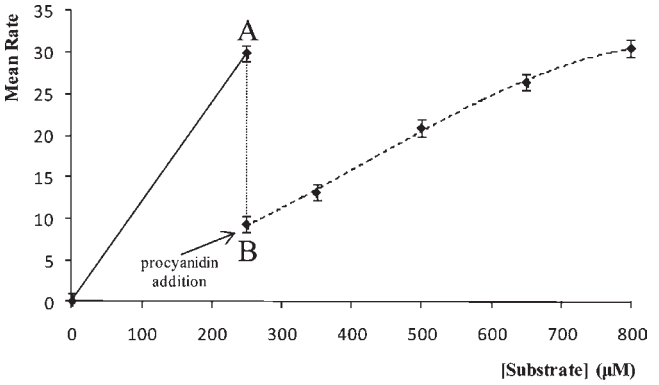

Figure 6. Kinetics of elastase (0.8 μM) with increasing concentrations of Suc-$(Ala)_3$-*p*-nitroanilide (0−800 μM) and using always the same OFP concentration (20 μM). Assays were conducted in 0.1 M phosphate buffer (pH 7.0) at 37 °C. The curve is an average of the triplicate analysis.

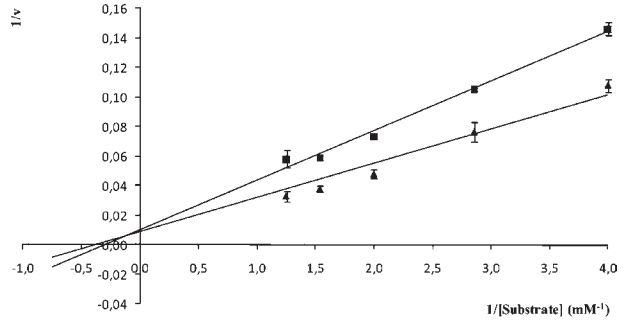

Figure 7. Representation of Lineweaver−Burk graphic in the absence of polyphenol inhibitor (▲) and in the presence of 20 μM of OFP (■). Assays were conducted with 0.8 μM of elastase in 0.1 M phosphate buffer (pH 7.0) at 37 °C.

activity. On the other hand, this data can also mean that polyphenols compete with the substrate for the active site, and in that case, the enzyme molecules remain active, whereas the reaction rate is slowed relatively to the rate in the absence of the procyanidins.

In order to study the affinity of each procyanidin to the active site of elastase under these conditions, the half maximal inhibitory concentration values (IC_{50}) for each compound were determined from **Figure 4** and are presented in **Table 1**. These values indicate that the procyanidin that needs the lowest concentration to inhibit half the maximal activity of elastase is the oligomeric fraction, while trimer C2 requires much higher concentrations for the same inhibition. However, IC_{50} values are not a direct indicator of affinity, thus the absolute inhibition constants (K_i) were calculated from the Cheng−Prusoff equation ($K_i = IC_{50}/(1 + [S]/K_m)$). Experimental binding free energies (ΔG_{exp}) for the substrate and each procyanidin studied were also calculated from the equations $\Delta G_{binding} = -RT \ln K_m$ and $\Delta G_{binding} = -RT \ln K_i$, respectively. The binding free energy value obtained for the Suc-$(Ala)_3$-*p*-nitroanilide substrate was −3.80 kcal/mol. The differences between the free

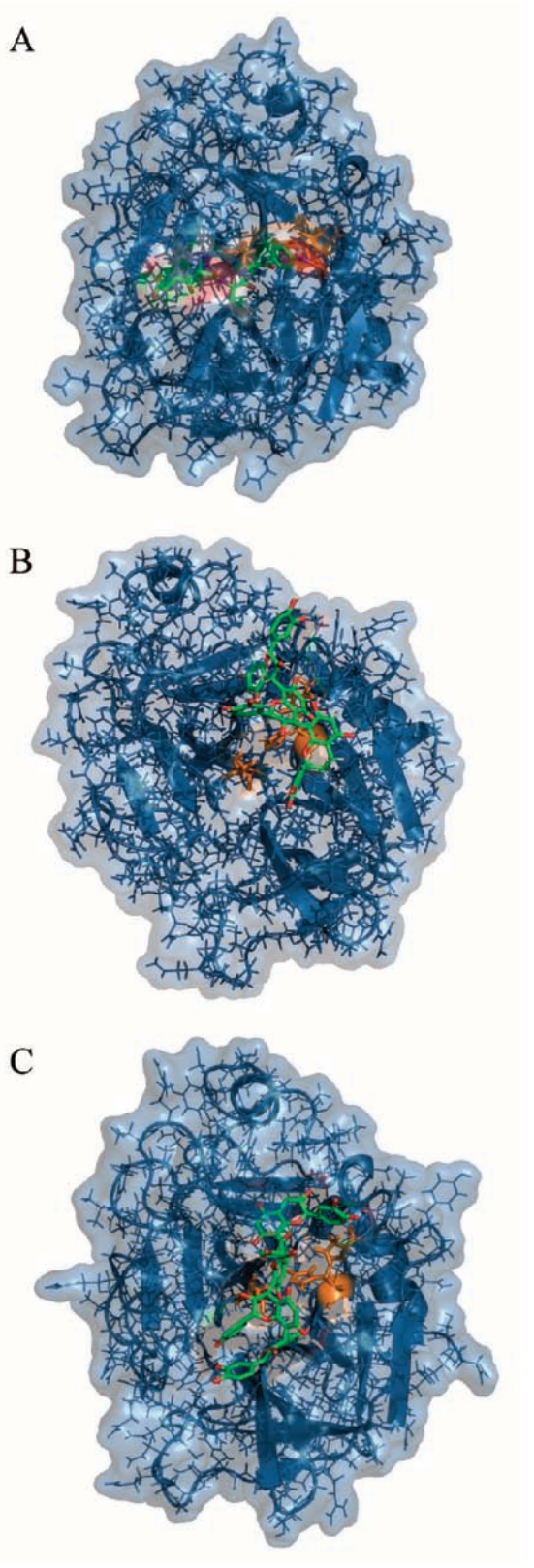

Figure 8. Representation of structures of the elastase:substrate (**A**), elastase:trimer (**B**) and elastase:tetramer (**C**) complexes. The substrate and procyanidins are colored at elements and the catalytic triad (His57, Asp102 and Ser195) is colored at orange.

energy values of each procyanidin related to the value obtained for the substrate ($\Delta\Delta G_{exp}$) were also calculated (**Table 1**).

It was observed that the most polymerized procyanidins possess the lower K_i value, which indicates a great affinity of

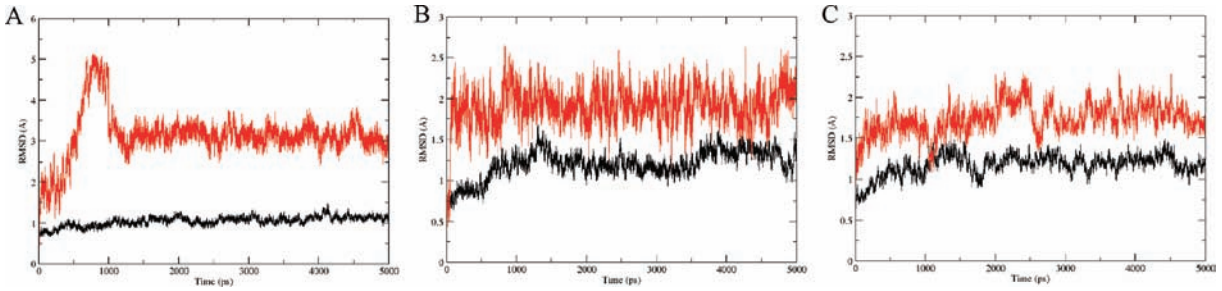

Figure 9. RMSD values obtained for the elastase backbone (black line) and for the Suc-$(Ala)_3$-*p*-nitroanilide substrate (red line, **A**), trimer (red line, **B**) and tetramer (red line, **C**).

these procyanidins to elastase, thus a higher inhibitory ability. Oppositely, the high K_i value obtained for trimer C2 demonstrates a weak affinity to the enzyme, which agrees with the small inhibitory effect (*circa* 10%) observed. Similar conclusions were obtained from the binding free energy values derived from K_i. Analyzing the $\Delta\Delta G_{exp}$, it is interesting to notice that trimer C2 shows a positive value, revealing a poorer affinity to the active site than the Suc-$(Ala)_3$-*p*-nitroanilide substrate used.

In order to investigate which kind of inhibition (reversible or irreversible) the addition of procyanidins causes, an assay with an addition of 20 μM of OFP was performed (**Figure 6**). Point A in **Figure 6** corresponds to the hydrolytic activity with 250 μM of substrate, point B indicates the inhibitory effect caused by the addition of procyanidins (20 μM) with the latter concentration of substrate, and the following points correspond to further addition of increasing concentrations of substrate. It was observed that the inhibitory effect at fixed procyanidin concentration decreases with increasing substrate concentrations.Thus, the inhibition caused by polyphenol compounds is reverted by further addition of substrate. These data indicate that both substrate and inhibitor molecules compete for the same active site, suggesting a competitive reversible inhibition. A competitive inhibitor binds reversibly with the enzyme to form an enzyme:inhibitor complex (EI), analogous to the enzyme:substrate complex (ES). In the presence of a competitive inhibitor, a higher substrate concentration is required to achieve its maximum velocity, thus the K_m value of the enzyme for substrate tends to increase, while V_{max} remains constant. **Figure 7** shows the Lineweaver−Burk plots, in the absence and presence of oligomeric fraction, and it was observed that both lines intercept the *y* axis in the same point, which indicate a similar value of V_{max}. This competition between the substrate and the polyphenol to the active site can justify the residual enzymatic activity previously referred, i.e. after the maximal inhibition activity, further addition of the inhibitor does not significantly change elastase activity. Oppositely, other authors such as Marina Carini et al. (2001) (*51*) and Roberto Facino et al. (1994) (*52*), have obtained a noncompetitive inhibition for the interaction between grape seed oligomers polyphenols and human neutrophils elastase (HNE). That discrepancy could be explained by the structural differences between elastin-cleaving enzymes (HNE and PPE) and also by the different composition of the oligomeric procyanidin fraction used herein (purified by chromatography) and the ones used by these authors (more complex grape seed extract).

Docking and Molecular Dynamics Studies. The binding of procyanidin molecules to elastase was simulated with docking and molecular dynamics methodologies. Due to the lack of crystallographic files of complexes between elastase and both the subtrate and procyanidins molecules, docking procedures using a distance constraint to the active site catalytic serine were performed. MD simulations were performed using the best docking solution for each compound as a starting structure.

Table 2. Distances of the Main Interactions between the Procyanidins (Trimer and Tetramer) and the Amino Acids of the Elastase Pocket

	elastase:trimer		elastase:tetramer	
residue	interaction	*d* (Å)	interaction	*d* (Å)
Tyr35			OH ↔ O (C ring)	2.96 ± 0.96
			apolar ring ↔ A-C ring	
Thr96	CO ↔ HO (D ring)	1.85 ± 0.19		
Asp98	COO^- ↔ HO (B ring)	2.40 ± 0.89		
Ala99	NH ↔ OH (B ring)	2.43 ± 0.35		
Gln192			NH_2 ↔ OH (I ring)	3.03 ± 1.28
Gly193			NH ↔ OH (E ring)	3.49 ± 0.58
Val216			CO ↔ HO (J ring)	1.96 ± 0.40
Arg217	NH_2 ↔ OH (A ring)	4.16 ± 0.82	NH_2 ↔ OH (F ring)	2.96 ± 0.99
Phe215	apolar ring ↔ E ring		apolar ring ↔ JL ring	

Figure 8 shows the structures that are closest to the average geometry of each complex. The root mean score deviation (RMSD) values for the protein backbone (Cα) and for each ligand (substrate, trimer and tetramer) during the MD simulations were obtained and are shown in the **Figure 9**. According to these results, it can be observed that RMSD values obtained for the protein backbone and substrate/trimer/tetramer are minimal, indicating the higher equilibration and stability of each complex.

The root mean score fluctuation (RMSF) values gives a measure of the movement of a subset of the system related to the average structure over the whole simulation (Figure SI-1 in Supporting Information). From the analysis of these RMSF values, it was possible to observe that, in the simulation with the substrate analogue, the residues Gly18, Asn132, Asn133, Arg145, Thr146, Asn147, and the three loops constituted by the 166−174, 184−188 and 217−224 residues, are the ones that mostly modify their position during the MD simulations. In the elastase:trimer simulation, the amino acids that show large changes in their 3D positions are Gln23, Arg24, Gly78, Ser26, Arg48, Gln49, Asn50, the 75−83, 109−119, 145−149 and 239−245 residues that constitute the flexible loops. However, in the elastase:tetramer simulation these flexible amino acids are Arg24, Asn25, Gly78, Thr79, the three loops constituted by the 113−120, 124−128 and 195−207 residues.

The RMSF values were also calculated for the substrate, trimer and tetramer molecules by atoms. According to the RMSF values obtained for the substrate molecule, it was observed that both extremities of the small peptide, i.e. the NO_2 group of the *p*-nitroanilide and the opposite carboxylic group, show higher flexibility and movement relatively to the average structure during the MD simulation process. Analyzing the trimeric procyanidin, it was observed that both rings E and H are highly flexible and present large fluctuations, while in the tetramer case, the hydroxyl groups of rings E, F, H, J, K and L are the only ones with more flexibility during the MD simulation.

The elastase is a digestive protease that specifically cleaves the peptidic bonds between small aliphatic amino acids as the binding

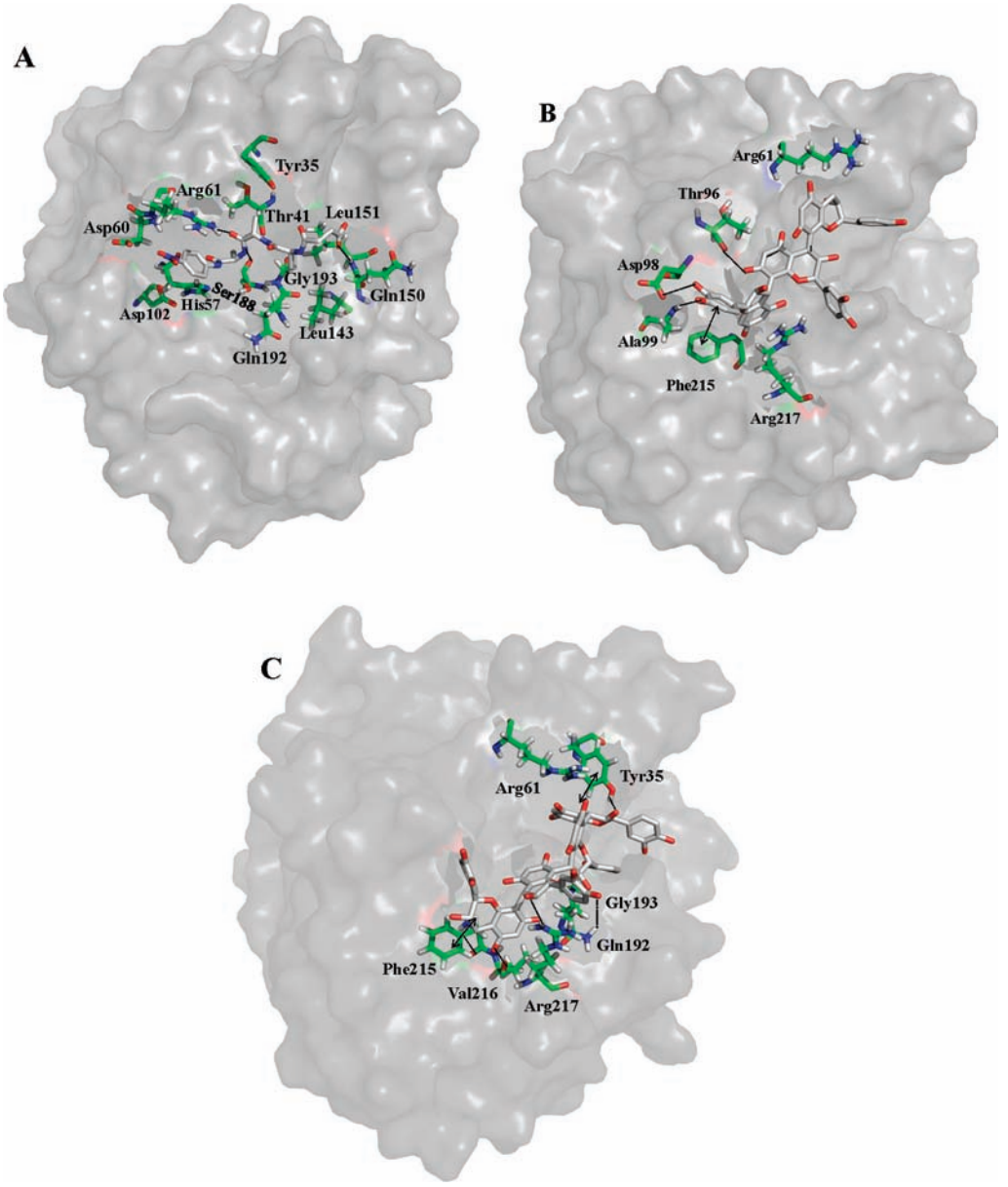

Figure 10. Representation of the main interactions established between the substrate (**A**), trimer (**B**) and tetramer (**C**) with the residues present close to active site of elastase. Substrate, trimer, tetramer and all residues are colored by element. The carbon atoms are green in the protein and gray for the ligands.

cavity (where the peptide chains are accommodated) is constituted mainly by residues with small aliphatic side chains. Structural information on the active site, in particular the hydrogen interactions established between the trimer and tetramer molecules and the neighbor amino acids, as well as van der Waals contacts established between the procyanidin rings and the aliphatic side chains of neighbor amino acids were analyzed and are shown in **Table 2**. As the substrate analogue used possesses three apolar alanines, this molecule establishes various hydrophobic contacts with the residues. However, it does not establish great hydrophilic interactions with the enzyme. The only exception is the short hydrogen interaction with the Leu141 with the average length of 2.39 ± 0.53 Å.

Figure 10 shows the main interactions established between the trimer and tetramer with elastase in the closest structure of the average geometry for both complexes.

In the complexes elastase:trimer and elastase:tetramer, it was seen that the main interactions occur via hydrogen bonds, particularly between the hydroxyl groups of the procyanidin rings and the Thr96, Asp98, Ala99, Arg217 and Tyr35, Gln192, Gly193, Val216, Arg217 residues, respectively. On the other hand, the presence of aromatic residues close to the active site provides the hydrophobic platform common to procyanidin−protein interactions. These amino acids display a position and orientation, which promotes the packing of the polyphenol rings during their binding. Moreover, the existence of several van der Waals contacts that are promoted by the aliphatic side chains present at the interface, namely, with Tyr35, His57 and Phe215, were also observed. It was noticed that the tetramer procyanidin establishes more contacts to the active site of elastase than the lower polymerized trimer compound, which is in agreement with the poorer affinity observed in the binding free energy obtained experimentally for the latter procyanidin. Furthermore, it is interesting to observe that the large side chains of both Arg61 and Arg217 are close to A−C and H rings plane of tetrameric procyanidin, respectively, which allows for a higher stabilization of this specific complex. It was noticed that both of these arginines are located close to the active site, and other studies have

suggested that Arg217 may be involved in substrate binding, as well as it was crucial for maintaining the active conformation of the enzyme (*50*).

In order to study the trimer and tetramer affinity for the active site of elastase, the theoretical values of the differences in the binding free energy values ($\Delta\Delta G_{theor}$) between the $\Delta G_{binding}$ obtained with elastase:trimer (4.7 kcal/mol) and elastase:tetramer (−10.5 kcal/mol) complexes to the $\Delta G_{binding}$ for the Suc-$(Ala)_3$-*p*-nitroanilide substrate were also calculated. Although these values are higher than the ones obtained experimentally, they are qualitatively and biologically similar. These values do not include the differential entropic contribution of the different ligands. However, they are expected to be much smaller than the values found for $\Delta\Delta G_{theor}$, thus they will not change the relative affinities calculated here. Therefore, the elastase:tetramer complexes display the most negative value of the binding free energy, which reveals the higher stability of this complex and the highest affinity of this procyanidin to the enzyme. Moreover, its formation is thermodynamically favored, and these results agree with the lower values of IC_{50} and K_i constants obtained experimentally for these complexes when compared to the elastase:trimer complexes.

In conclusion, activity measurements of the porcine pancreatic elastase (PPE) have been performed to know the kinetic parameters using the Suc-$(Ala)_3$-*p*-nitroanilide as substrate and procyanidins as inhibitors. A decrease in proteolysis activity with addition of increasing polyphenol concentrations was observed. Considering that the order of inhibitory ability obtained was OFP > tetramer > trimer procyanidins, we can conclude that the inhibitory effect increases with increasing molecular weight of procyanidins. It was shown that more polymerized procyanidins establish stronger intermolecular interactions with the amino acids present on elastase active site, thus have higher inhibitory ability than the smaller ones. Therefore, it can be concluded that procyanidins with molecular weight of at least 1154 Da are necessary for significant inhibition ability. Kinetic parameters were also calculated, and it was concluded that the polyphenols' inhibition of elastase is reversible and competitive.

Molecular docking and dynamics simulations demonstrated that short hydrogen bonds and van der Waals interactions established between the tetramer groups and the side chains of residues present on elastase active site stabilize and favor the binding of this procyanidin. The experimental and theoretical differences in the binding free energy values ($\Delta\Delta G$) were also calculated, and both results are qualitatively and biologically similar. The complex with the tetramer displays the most negative value, revealing that its formation is thermodynamically favored when compared with the complexes elastase:substrate and elastase:trimer.

In general, elastase inhibition by procyanidins may contribute to a reduction in the proteolysis of proteins that may allow a reduced weight gain in animals. It also may contribute to longer digestion times, leading to a sensation of fullness that may reduce overall food intake, contributing to control obesity. Furthermore, these results may be relevant to study new elastase inhibitors for therapeutic purposes like pulmonary emphysema, acute pancreatitis, rheumatoid arthritis and thrombosis.

Supporting Information Available: RMSF values obtained for the elastase by residues complexed with Suc-$(Ala)_3$-*p*-nitroanilide substrate, trimer C2 and tetramer molecules (Figure SI-1). This material is available free of charge via the Internet at http://pubs.acs.org.

LITERATURE CITED

(1) Santos-Buelga, C.; Scalbert, A. Proanthocyanidins and tannin-like compounds - nature, occurrence, dietary intake and effects on nutrition and health. *J. Sci. Food Agric.* **2000**, *80*, 1094−1117.

(2) Xue, Z. P.; Feng, W. H.; Cao, J. K.; Cao, D. D.; Jiang, W. B. Antioxidant activity and total phenolic contents in peel and pulp of chinese jujube (ziziphus jujuba mill) fruits. *J. Food Biochem.* **2009**, *33*, 613−629.

(3) Daniel, K. G.; Landis-Piwowar, K. R.; Chen, D.; Wan, S. B.; Chan, T. H.; Dou, Q. P. Methylation of green tea polyphenols affects their binding to and inhibitory poses of the proteasome beta 5 subunit. *Int. J. Mol. Med.* **2006**, *18*, 625−632.

(4) Pezzato, E.; Sartor, L.; Dell Aica, I.; Dittadi, R.; Gion, M.; Belluco, C.; Lise, M.; Garbisa, S. Prostate carcinoma and green tea: Psa-triggered basement membrane degradation and mmp-2 activation are inhibited by (-)epigallocatechin-3-gallate. *Int. J. Cancer* **2004**, *112*, 787−792.

(5) Herrero-Martinez, J. M.; Sanmartin, M.; Roses, M.; Bosch, E.; Rafols, C. Determination of dissociation constants of flavonoids by capillary electrophoresis. *Electrophoresis* **2005**, *26*, 1886−1895.

(6) Justino, G. C.; Borges, C. M.; Florencio, M. H. Electrospray ionization tandem mass spectrometry fragmentation of protonated flavone and flavonol aglycones: A re-examination. *Rapid Commun. Mass Spectrom.* **2009**, *23*, 237−248.

(7) McDougall, G. J.; Stewart, D. The inhibitory effects of berry polyphenols on digestive enzymes. *Biofactors* **2005**, *23*, 189−195.

(8) Sengupta, B.; Sengupta, P. K. Binding of quercetin with human serum albumin: A critical spectroscopic study. *Biopolymers* **2003**, *72*, 427−434.

(9) Dufour, C.; Dangles, O. Flavonoid-serum albumin complexation: Determination of binding constants and binding sites by fluorescence spectroscopy. *Biochim. Biophys. Acta* **2005**, *1721*, 164−173.

(10) Papadopoulou, A.; Green, R. J.; Frazier, R. A. Interaction of flavonoids with bovine serum albumin: A fluorescence quenching study. *J. Agric. Food Chem.* **2005**, *53*, 158−163.

(11) de Freitas, V.; Carvalho, E.; Mateus, N. Study of carbohydrate influence on protein-tannin aggregation by nephelometry. *Food Chem.* **2003**, *81*, 503−509.

(12) Dell'Aica, I.; Niero, R.; Piazza, F.; Cabrelle, A.; Sartor, L.; Colalto, C.; Brunetta, E.; Lorusso, G.; Benelli, R.; Albini, A.; Calabrese, F.; Agostini, C.; Garbisa, S. Hyperforin blocks neutrophil activation of matrix metalloproteinase-9, motility and recruitment, and restrains inflammation-triggered angiogenesis and lung fibrosis. *J. Pharmacol. Exp. Ther.* **2007**, *321*, 492−500.

(13) Sartor, L.; Pezzato, E.; Dell'Aica, I.; Caniato, R.; Biggin, S.; Garbisa, S. Inhibition of matrix-proteases by polyphenols: Chemical insights for anti-inflammatory and anti-invasion drug design. *Biochem. Pharmacol.* **2002**, *64*, 229−237.

(14) Smith, D. M.; Daniel, K. G.; Wang, Z. G.; Guida, W. C.; Chan, T. H.; Dou, Q. P. Docking studies and model development of tea polyphenol proteasome inhibitors: Applications to rational drug design. *Proteins* **2004**, *54*, 58−70.

(15) Luck, G.; Liao, H.; Murray, N. J.; Grimmer, H. R.; Warminski, E. E.; Williamson, M. P.; Lilley, T. H.; Haslam, E. Polyphenols, astringency and proline-rich proteins. *Phytochemistry* **1994**, *37*, 357−371.

(16) Baxter, N. J.; Lilley, T. H.; Haslam, E.; Williamson, M. P. Multiple interactions between polyphenols and a salivary proline-rich protein repeat result in complexation and precipitation. *Biochemistry* **1997**, *36*, 5566−5577.

(17) Simon, C.; Barathieu, K.; Laguerre, M.; Schmitter, J. M.; Fouquet, E.; Pianet, I.; Dufourc, E. J. Three-dimensional structure and dynamics of wine tannin-saliva protein complexes. A multitechnique approach. *Biochemistry* **2003**, *42*, 10385−10395.

(18) Frazier, R. A.; Papadopoulou, A.; Mueller-Harvey, I.; Kissoon, D.; Green, R. J. Probing protein-tannin interactions by isothermal titration microcalorimetry. *J. Agric. Food Chem.* **2003**, *51*, 5189−5195.

(19) Goncalves, R.; Soares, S.; Mateus, N.; De Freitas, V. Inhibition of trypsin by condensed tannins and wine. *J. Agric. Food Chem.* **2007**, *55*, 7596−7601.

(20) Horne, J.; Hayes, J.; Lawless, H. T. Turbidity as a measure of salivary protein reactions with astringent substances. *Chem. Senses* **2002**, *27*, 653−659.

(21) Nadarajah, D.; Atkinson, M. A. L.; Huebner, P.; Starcher, B. Enzyme kinetics and characterization of mouse pancreatic elastase. *Connect. Tissue Res.* **2008**, *49*, 409−415.

(22) Wurtele, M.; Hahn, M.; Hilpert, K.; Hohne, W. Atomic resolution structure of native porcine pancreatic elastase at 1.1 angstrom. *Acta Crystallogr., Sect. D: Biol. Crystallogr.* **2000**, *56*, 520−523.

(23) Berglund, G. I.; Smalas, A. O.; Outzen, H.; Willassen, N. P. Purification and characterization of pancreatic elastase from north atlantic salmon (salmo salar). *Mol. Marine Biol. Biotechnol.* **1998**, *7*, 105−114.

(24) Wright, P. A.; Wilmouth, R. C.; Clifton, I. J.; Schofield, C. J. Kinetic and crystallographic analysis of complexes formed between elastase and peptides from beta-casein. *Eur. J. Biochem.* **2001**, *268*, 2969−2974.

(25) Bras, N. F.; Goncalves, R.; Fernandes, P. A.; Mateus, N.; Ramos, M. J.; de Freitas, V. Understanding the binding of procyanidins to pancreatic elastase by experimental and computational methods. *Biochemistry* **2010**, *49*, 5097−5108.

(26) Geissman, T. A.; Yoshimura, N. N. Synthetic proanthocyanidin. *Tetrahedron Lett.* **1966**, *7*, 2669−2673.

(27) Delcour, J. A.; Ferreira, D.; Roux, D. G. Synthesis of condensed tannins. Part 9. The condensation sequence of leucocyanidin with (+)-catechin and with the resultant procyanidins. *J. Chem. Soc., Perkin Trans. 1* **1983**, 1711−1717.

(28) Tarascou, I.; Barathieu, K.; Simon, C.; Ducasse, M. A.; Andre, Y.; Fouquet, E.; Dufourc, E. J.; de Freitas, V.; Laguerre, M.; Pianet, I. A 3d structural and conformational study of procyanidin dimers in water and hydro-alcoholic media as viewed by nmr and molecular modeling. *Magn. Reson. Chem.* **2006**, *44*, 868−880.

(29) Tarascou, I.; Ducasse, M. A.; Dufourc, E. J.; Moskau, D.; Fouquet, E.; Laguerre, M.; Pianet, I. Structural and conformational analysis of two native procyanidin trimers. *Magn. Reson. Chem.* **2007**, *45*, 157−166.

(30) de Freitas, V.; Glories, Y.; Bourgeois, G.; Vitry, C. Characterisation of oligomeric and polymeric procyanidins from grape seeds by liquid secondary ion mass spectrometry. *Phytochemistry* **1998**, *49*, 1435−1441.

(31) González-Manzano, S.; Mateus, N.; de Freitas, V.; Santos-Buelga, C. Influence of the degree of polymerisation in the ability of catechins to act as anthocyanin copigments. *Eur. Food Res. Technol.* **2008**, *227*, 83−92.

(32) Steuerwald, A. J.; Villeneuve, J. D.; Sun, L.; Stenken, J. A. In vitro characterization of an in situ microdialysis sampling assay for elastase activity detection. *J. Pharm. Biomed. Anal.* **2006**, *40*, 1041−1047.

(33) Geller, M.; Swanson, S. M.; Meyer, E. F. Dynamic properties of the 1st steps of the enzymatic-reaction of porcine pancreatic elastase (ppe) 0.2. Molecular-dynamics simulation of a michaelis complex-ppe and the hexapeptide thr-pro-nval-leu-tyr-thr. *J. Am. Chem. Soc.* **1990**, *112*, 8925−8931.

(34) Wilmouth, R. C.; Edman, K.; Neutze, R.; Wright, P. A.; Clifton, I. J.; Schneider, T. R.; Schofield, C. J.; Hajdu, J. X-ray snapshots of serine protease catalysis reveal a tetrahedral intermediate. *Nat. Struct. Biol.* **2001**, *8*, 689−694.

(35) Sreenivasan, U.; Axelsen, P. H. Buried water in homologous serine proteases. *Biochemistry* **1992**, *31*, 12785−12791.

(36) Jones, G.; Willett, P.; Glen, R. C.; Leach, A. R.; Taylor, R. Development and validation of a genetic algorithm for flexible docking. *J. Mol. Biol.* **1997**, *267*, 727−748.

(37) Verdonk, M. L.; Cole, J. C.; Hartshorn, M. J.; Murray, C. W.; Taylor, R. D. Improved protein-ligand docking using gold. *Proteins* **2003**, *52*, 609−623.

(38) Frisch, M. J., Trucks, G. W.; Schlegel, H. B.; Scuseria, G. E.; Robb, M. A.; Cheeseman, J. R.; Zakrzewski, V. G.; Montgomery, J. A., Jr.; Stratmann, R. E.; Burant, J. C.; Dapprich, S.; Millam, J. M.; Daniels, A. D.; Kudin, K. N.; Strain, M. C.; Farkas, O.; Tomasi, J.; Barone, V.; Cossi, M.; Cammi, R.; Mennucci, B.; Pomelli, C.; Adamo, C.; Clifford, S.; Ochterski, J.; Petersson, G. A.; Ayala, P. Y.; Cui, Q.; Morokuma, K.; Malick, D. K.; Rabuck, D. A.; Raghavachari, K.; Foresman, J. B.; Cioslowski, J.; Ortiz, J. V.; Baboul, A. G.; Stefanov, B. B.; Liu, G.; Liashenko, A.; Piskorz, P.; Komaromi, I.; Gomperts, R.; Martin, R. L.; Fox, D. J.; Keith, T.; Al-Laham, M. A.; Peng, C. Y.; Nanayakkara, A.; Gonzalez, C.; Challacombe, M.; Gill, P. M. W.; Johnson, B.; Chen, W.; Wong, M. W.; Andres, J. L.; Gonzalez, C.; Head-Gordon, M.; Replogle, E. S.; Pople, J. A. *Gaussian 03*, revision D.01/D.02; Gaussian, Inc.: Pittsburgh, PA, 2003.

(39) Bayly, C. I.; Cieplak, P.; Cornell, W. D.; Kollman, P. A. A well-behaved electrostatic potential based method using charge restraints for deriving atomic charges - the resp model. *J. Phys. Chem.* **1993**, *97*, 10269−10280.

(40) Case, D. A.; Cheatham, T. E.; Darden, T.; Gohlke, H.; Luo, R.; Merz, K. M.; Onufriev, A.; Simmerling, C.; Wang, B.; Woods, R. J. The amber biomolecular simulation programs. *J. Comput. Chem.* **2005**, *26*, 1668−1688.

(41) Izaguirre, J. A.; Catarello, D. P.; Wozniak, J. M.; Skeel, R. D. Langevin stabilization of molecular dynamics. *J. Chem. Phys.* **2001**, *114*, 2090−2098.

(42) Case, D. A.; Darden, T. A.; Cheatham, T. E., III; Simmerling, C. L.; Wang, J.; Duke, R. E.; Luo, R.; Crowley, M.; Walker, R. C.; Zhang, W.; Merz, K. M.; Wang, B.; Hayik, S.; Roitberg, A.; Seabra, G.; Kolossváry, I.; Wong, K. F.; Paesani, F.; Vanicek, J.; Wu, X.; Brozell, S. R.; Steinbrecher, T.; Gohlke, H.; Yang, L.; Tan, C.; Mongan, J.; Hornak, V.; Cui, G.; Mathews, D. H.; Seetin, M. G.; Sagui, C.; Babin, V.; Kollman, P. A. *Amber 10*; University of California: San Francisco, 2008.

(43) Cornell, W. D.; Cieplak, P.; Bayly, C. I.; Gould, I. R.; Merz, K. M.; Ferguson, D. M.; Spellmeyer, D. C.; Fox, T.; Caldwell, J. W.; Kollman, P. A. A 2nd generation force-field for the simulation of proteins, nucleic-acids, and organic-molecules. *J. Am. Chem. Soc.* **1995**, *117*, 5179−5197.

(44) Ryckaert, J. P.; Ciccotti, G.; Berendsen, H. J. C. Numerical-integration of cartesian equations of motion of a system with constraints - molecular-dynamics of n-alkanes. *J. Comput. Phys.* **1977**, *23*, 327−341.

(45) Huo, S.; Massova, I.; Kollman, P. A. Computational alanine scanning of the 1: 1 human growth hormone-receptor complex. *J. Comput. Chem.* **2002**, *23*, 15−27.

(46) Rocchia, W.; Alexov, E.; Honig, B. In *Extending the applicability of the nonlinear Poisson-Boltzmann equation: Multiple dielectric constants and multivalent ions*, Symposium on Molecular Dynamics - The Next Millennium, New York, NY, June 2−3, 2000; New York, NY, 2000; pp 6507−6514.

(47) Rocchia, W.; Sridharan, S.; Nicholls, A.; Alexov, E.; Chiabrera, A.; Honig, B. Rapid grid-based construction of the molecular surface and the use of induced surface charge to calculate reaction field energies: Applications to the molecular systems and geometric objects. *J. Comput. Chem.* **2002**, *23*, 128−137.

(48) Moreira, I. S.; Fernandes, P. A.; Ramos, M. J. Accuracy of the numerical solution of the poisson-boltzmann equation. *THEOCHEM* **2005**, *729*, 11−18.

(49) Connolly, M. L. Analytical molecular-surface calculation. *J. Appl. Crystallogr.* **1983**, *16*, 548−558.

(50) Davril, M.; Jung, M. L.; Duportail, G.; Lohez, M.; Han, K. K.; Bieth, J. G. Arginine modification in elastase - effect on catalytic activity and conformation of the calcium-binding site. *J. Biol. Chem.* **1984**, *259*, 3851−3857.

(51) Carini, M.; Stefani, R.; Aldini, G.; Ozioli, M.; Facino, R. M. Procyanidins from vitis vinifera seeds inhibit the respiratory burst of activated human neutrophils and lysosomal enzyme release. *Planta Med.* **2001**, *67*, 714−717.

(52) Facino, R. M.; Carini, M.; Aldini, G.; Bombardelli, E.; Morazzoni, P.; Morelli, R. Free-radicals scavenging action and anti-enzyme activities of procyanidines from vitis-vinifera - a mechanism for their capillary protective action. *Arzneim. Forsch.* **1994**, *44−1*, 592−601.

Received for review May 12, 2010. Revised manuscript received September 1, 2010. Accepted September 2, 2010. The authors would like to thankfully acknowledge the research project grant (PTDC/AGR-ALI/67579/2006) funding from FCT (Fundação para a Ciência e Tecnologia) from Portugal. N.F.B. and R.G. would like to thankfully acknowledge PhD grants by FCT (SFRH/BD/31359/2006 and SFRH/BD/38814/2007, respectively).